

Bistable Copper Complexes of Bis-thia-bis-quinoline Ligands

Valeria Amendola,[†] Carlo Mangano,[†] Piersandro Pallavicini,^{*†} and Michele Zema[‡]*Dipartimento di Chimica Generale, Università di Pavia, v. Taramelli, 12–27100 Pavia, Italy, and Centro Grandi Strumenti, Università di Pavia, v. Bassi, 6–27100 Pavia, Italy*

Received May 2, 2002

The new ligands *R,R-trans-S,S'*-bis[methyl(2'-quinoly)]-1,2-dithiacyclohexane, *cis-S,S'*-bis[methyl(2'-quinoly)]-1,2-dithiacyclohexane, and 1,6-bis(2'-quinoly)-2,5-dithiahexane have been synthesized and their complexes with Cu^I and Cu^{II} prepared. The ligand/metal systems are bistable, as the complexes with copper in both its oxidation states are stable under the same conditions as solids and in solution. The crystal and molecular structure of [Cu^I(1,6-bis(2'-quinoly)-2,5-dithiahexane)]ClO₄ has been determined by X-ray diffraction and reveals that the complex is monomeric, with the ligand folding around the Cu⁺ cation, imparting to it a tetrahedral coordination. UV–vis, MS–ESI, and NMR data indicate that the same is found for the Cu^I complexes of all three ligands. Also, the Cu^{II} complexes are monomeric, but with a square arrangement of the ligands around Cu²⁺. On changing the oxidation state, the change in the geometrical arrangement is fast and complete in less than 80 ms, as demonstrated by cyclic voltammetry experiments. In the CV profiles, the oxidation and reduction events take place at separated E_{ox} and E_{red} values, with no return wave even at the fastest scan rates. In the E_{ox} – E_{red} interval (which ranges from 450 to 650 mV, depending on the ligand), the ligand/copper system can thus exist in one of its two states, depending on its history, and thus display electrochemical hysteretic behavior. The electrochemical cycle leading from the tetrahedral [Cu^I(ligand)]⁺ to the square [Cu^{II}(ligand)]²⁺ complex (and vice versa) is reversible and repeatable without degradation, as checked by coupled UV–vis-controlled potential coulometry experiments.

Introduction

Copper offers two oxidation states of comparable stability, I and II, and may easily form bistable systems if coordinated by ligands featuring a donor set capable of advantageously interacting with both Cu^I and Cu^{II}.¹ Moreover, Cu^I prefers four-coordination with a tetrahedral geometry, and Cu^{II} prefers five-coordination (either with a square-pyramidal or a trigonal-bipyramidal geometry) or six-coordination, with a very elongated tetragonal geometry. This often leads to such significant differences between Cu^{II} and Cu^I in the metal/ligand geometry and molecular overall shape that, on changing oxidation state, the whole system behaves as a

molecular machine, whose components can be made to move electrochemically or by means of a chemical redox reaction.² In some cases, these copper-based systems display an even more valuable property, i.e., hysteresis,³ which opens the path to the possibility of storing information at a molecular level.^{3f,4} In particular, the electrochemically driven self-assembling/disassembling of metal helicates has been described with systems based on the Cu^{II}/Cu^I couple and on ligands **1–3**, which contain a bis-imino-bis-heterocycle donor set and display a fair affinity for both oxidation states of copper.⁵ Ligands **1–3** coordinate Cu^{II} arranging around it

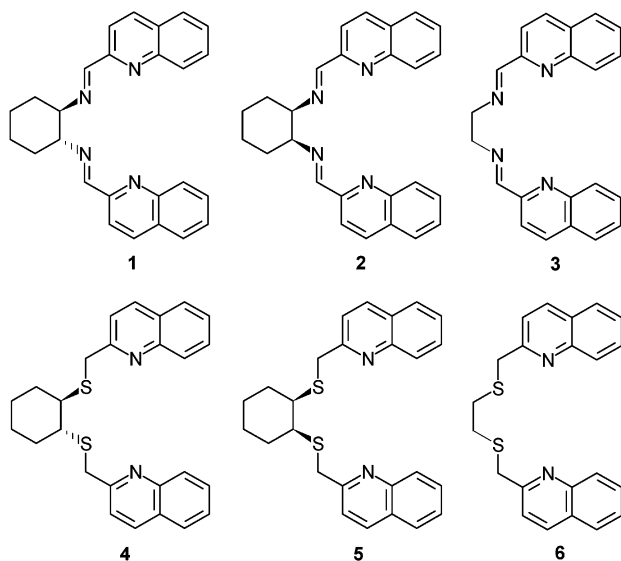
* To whom correspondence should be addressed. E-mail: psp@unipv.it.

[†] Dipartimento di Chimica Generale.[‡] Centro Grandi Strumenti.

- (1) (a) Burke, P. J.; Henrick, K.; McMillin, D. R. *Inorg. Chem.* **1982**, *21*, 1881. (b) Goodwin, J. A.; Bodager, G. A.; Wilson, L. J.; Stanbury, D. M.; Scheidt, W. R. *Inorg. Chem.* **1989**, *28*, 35. (c) Coggin, D. K.; Gonzales, J. A.; Kook, A. M.; Stanbury, D. M.; Wilson, L. J. *Inorg. Chem.* **1991**, *30*, 1115. (d) Coggin, D. K.; Gonzales, J. A.; Kook, A. M.; Bergman, C.; Brennan, T. D.; Scheidt, W. R.; Stanbury, D. M.; Wilson, L. J. *Inorg. Chem.* **1991**, *30*, 1125. (e) Knapp, S.; Keenan, T. P.; Zhang, X.; Fikar, R.; Potenza, J. A.; Schugar, H. J. *J. Am. Chem. Soc.* **1990**, *112*, 3452.

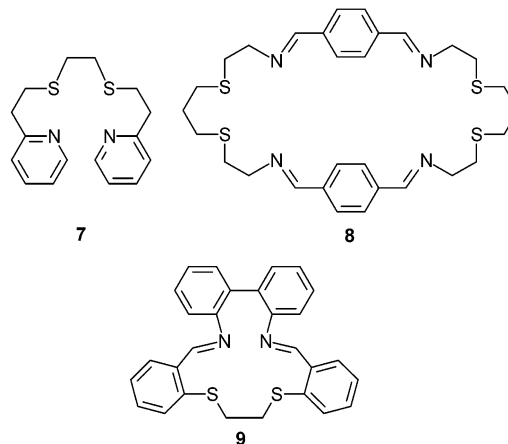
- (2) (a) Rahem, L.; Sauvage, J.-P. In *Struct. Bonding*; Sauvage, J.-P., Ed.; Springer-Verlag: Berlin, 2001; vol 99, p 55. (b) Balzani, V.; Credi, A.; Raymo, F. M.; Stoddart, J. F. *Angew. Chem., Int. Ed.* **2000**, *39*, 3349. (c) Chambron, J.-C. In *Perspective in Supramolecular Chemistry*; Sauvage, J.-P., Ed.; John Wiley & Sons: Chichester, U.K., 1999; vol. 5, p 225.
- (3) (a) Kahn, O.; Launay, J. P. *Chemtronics* **1988**, *3*, 140. (b) Bolvin, H.; Khan, O.; Vekhter, B. *New J. Chem.* **1991**, *15*, 889. (c) Connelly, N. G.; Raven, S. J.; Carriedo, G. A.; Riera, V. *J. Chem. Soc., Chem. Commun.* **1986**, 992. (d) Vallat, A.; Person, M.; Roullier, L.; Laviron, E. *Inorg. Chem.* **1987**, *26*, 332. (e) Sano, M.; Taube, H. *J. Am. Chem. Soc.* **1991**, *113*, 2327. (f) Sano M. In *Struct. Bonding*; Sauvage, J.-P., Ed.; Springer-Verlag: Berlin 2001; vol 99, p 117.
- (4) Amendola, A.; Fabbri, L.; Gianelli, L.; Maggi, C.; Mangano, C.; Pallavicini, P.; Zema, M. *Inorg. Chem.* **2001**, *40*, 3579.

with a square planar geometry and forming monomeric complexes, while with Cu^{I} a single ligand, due to its rigidity, is not able to fold and arrange around the metal cation with a tetrahedral geometry. According to this, two ligands have to couple with two Cu^{I} cations in order to satisfy the coordination requirements of the latter, and dimeric helical complexes are obtained. The two possible states of the system (helical dimer and square planar monomer) can be interconverted electrochemically, with electrochemical profiles which display hysteresis.⁴ In order to try to increase the set of systems capable of displaying electrochemical hysteresis, we have prepared the new ligands **4–6**, in which the same frame of ligands **1–3** has been maintained, but the donor set has been modified, changing the two imino groups into two thioether donor atoms.



The bis-thia-bis-quinoline donor set appears capable of favorably interacting with both Cu^{II} and Cu^{I} , as suggested by the reported examples of ligands containing a similar donor set and forming stable complexes with both oxidation states of copper. These ligands include a bis-thia-bis-pyridine ligand, **7**,⁶ and macrocyclic ligands containing bis-thia-bis-imine donor sets such as **8**⁷ and **9**.⁸ Different from the copper complexes of **1–3**, these systems are coordination number invariant with the redox change, being monomeric and with the four donors bound to the metal center with both Cu^{I} and Cu^{II} . However, serious geometrical rearrangements in the overall complex structure are observed on changing the oxidation state, following the change in the geometry of the four donors around the copper cation. In this paper, we report the synthesis of ligands **4–6** and of their Cu^{I} and Cu^{II}

complexes, whose structure as been investigated in the solid state and in solution. The obtained complexes are monomeric in both oxidation states. The systems are bistable as $[\text{Cu}^{\text{II}}(\text{ligand})]^{2+}/[\text{Cu}^{\text{I}}(\text{ligand})]^+$ are stable under the same conditions and can be electrochemically interconverted. Moreover, electrochemistry indicates for all systems an hysteresis-like behavior.



Experimental Section

Synthesis of the Ligands. Ligands **4–6** were prepared from *R,R*-*trans*-1,2-cyclohexanedithiol,⁹ *cis*-1,2-cyclohexanedithiol,¹⁰ 1,2-ethanedithiol,¹⁰ and 2-chloromethylquinoline (Aldrich product) according to the same procedure, which is described in the following lines. To 25 mL of absolute ethanol was added 8 mmol of sodium, and the mixture was allowed to react under a nitrogen atmosphere. When all the sodium metal had dissolved, 4 mmol of the chosen dithiol was added and stirred at 40 °C for 30 min. To the obtained solution, 8 mmol of 2-chloromethylquinoline dissolved in 7 mL of absolute ethanol was added. The reaction mixture was then heated at reflux temperature for 20 h, then cooled, and filtered, and the solvent removed on a rotary evaporator. The residue was redissolved with 50 mL of CH_2Cl_2 and the organic phase washed with 50 mL of water and dried over Na_2SO_4 . After drying, the desiccant was removed by filtration, the solvent evaporated on a rotary evaporator, and the crude product purified by chromatography on a SiO_2 column with *n*-hexane/ethyl acetate (gradient from 9:1 to 5:1 v/v) as eluent.

***R,R*-*trans*-*S,S'*-Bis[methyl(2'-quinolyl)]-1,2-dithiacyclohexane (4).** This compound is a waxy yellowish solid, $\text{C}_{26}\text{H}_{26}\text{N}_2\text{S}_2$. Yield: 38%. MS-ESI: $m/z = 453$ (**4** + Na^+). ^1H NMR (CD_3CN): $\delta = 8.20$ (d, 2H) + 7.83 (d, 2H) + 7.78 (d, 2H) + 7.62 (t, 2H) + 7.5 (d + t, 4H), H of the quinoline rings; 3.98 (s, 4H, SCH_2 -quinoline); 2.93 (m, 2H, (S)CHCH(S) of the cyclohexane ring); 1.6–1.3 (m, 8H, CH_2 of the cyclohexane ring).

***cis*-*S,S'*-Bis[methyl(2'-quinolyl)]-1,2-dithiacyclohexane (5).** This compound is a waxy yellowish solid, $\text{C}_{26}\text{H}_{26}\text{N}_2\text{S}_2$. Yield: 33%. MS-ESI: $m/z = 431$ (**5** + H^+). ^1H NMR (CD_3CN): $\delta = 8.19$ (d, 2H) + 7.81 (d, 2H) + 7.79 (d, 2H) + 7.68 (t, 2H) + 7.53 (t, 2H) + 7.46 (d, 2H), H of the quinoline rings; 3.91 (m, 4H, SCH_2 -quinoline); 3.12 (m, 2H, (S)CHCH(S) of the cyclohexane ring); 1.8–1.3 (m, 8H, CH_2 of the cyclohexane ring).

1,6-Bis(2'-quinolyl)-2,5-dithiahexane (6). This compound is a yellowish solid, $\text{C}_{22}\text{H}_{20}\text{N}_2\text{S}_2$. Yield: 25%. MS-ESI: $m/z = 377$ (**6** + H^+). ^1H NMR (CD_3CN): $\delta = 8.21$ (d, 2H) + 7.94 (d, 2H) +

(5) (a) Amendola, A.; Fabbri, L.; Pallavicini, P. *Coord. Chem. Rev.* **2001**, 216–217, 435. (b) Amendola, A.; Fabbri, L.; Linati, L.; Mangano, P.; Pallavicini, P.; Pedrazzini, V.; Zema, M. *Chem. Eur. J.* **1999**, 5, 3679.

(6) Brubaker, G. R.; Brown, J. N.; Yoo, M. K.; Kinsey, R. A.; Kutchan, T. M.; Mottel, E. A. *Inorg. Chem.* **1979**, 18, 299.

(7) Comba, P.; Fath, A.; Hambley, T. W.; Richens, D. T. *J. Chem. Soc., Chem. Commun.* **1995**, 1883.

(8) Flanagan, S.; Dung, J.; Haller, K.; Wang, S.; Scheidt, W. R.; Scott, R. A.; Webb, T. R.; Stanbury, D. M.; Wilson, L. J. *J. Am. Chem. Soc.* **1997**, 119, 8857.

(9) Iqbal, S. M.; Owen, N. L. *J. Chem. Soc.* **1960**, 1030.

(10) Howl, J.; Whitesides, G. M. *J. Am. Chem. Soc.* **1987**, 109, 6825.

7.89 (d, 2H) + 7.72 (t, 2H) + 7.57 (t, 2H) + 7.52 (d, 2H), H of the quinoline rings; 3.99 (s, 4H, SCH₂-quinoline); 2.72 (s, 4H, SCH₂CH₂S).

Synthesis of the Copper Complexes. Cu^I and Cu^{II} complexes of ligands **4–6** have been obtained by treating 50 mg of the chosen ligand, dissolved in 10 mL of acetonitrile, with the stoichiometric amount of anhydrous, solid [Cu^I(CH₃CN)₄]ClO₄ or Cu^{II}(CF₃SO₃)₂, under a nitrogen atmosphere. The solid complexes precipitated from the solutions as crystals or microcrystalline powders, by slow diffusion of diethyl ether.

[Cu^I(*R,R*-*trans*-*S,S'*-bis[methyl(2'-quinolyl)]-1,2-dithiacyclohexane)]ClO₄, [Cu^I(**4**)]ClO₄. This compound is a bright-yellow microcrystalline solid, yield 91%. Anal. Calcd, for C₂₆H₂₆ClCuN₂O₄S₂: C 52.61, H 4.41, N 4.72%. Found: C 52.52, H 4.45, N 4.80. Mass spectra (MS-ESI, on an acetonitrile solution of a redissolved solid sample): *m/z* 493, 495 for [Cu(**4**)]⁺. ¹H NMR (CD₃CN): δ = 8.56 (d, 2H) + 8.32 (d, 2H) + 8.11 (t, 2H) + 7.75–7.65 (m, 6H), H of the quinoline rings; 4.70 (m, 4H, SCH₂-quinoline); 2.64 (m, 2H, (S)CHCH(S) of the cyclohexane ring); 1.8–0.9 (m, 8H, CH₂ of the cyclohexane ring).

[Cu^{II}(*R,R*-*trans*-*S,S'*-bis[methyl(2'-quinolyl)]-1,2-dithiacyclohexane)](CF₃SO₃)₂, [Cu^{II}(**4**)](CF₃SO₃)₂. This compound is a deep-green powder, yield 79%. Anal. Calcd, for C₂₈H₂₆CuF₆N₂O₆S₄: C 39.43, H 3.31, N 3.54%. Found: C 39.39, H 3.35, N 3.59%. Mass spectra (MS-ESI, on an acetonitrile solution of a redissolved solid sample): *m/z* 642, 644 for {[Cu(**4**)](CF₃SO₃)⁺}.⁺

[Cu^I(*cis*-*S,S'*-bis[methyl(2'-quinolyl)]-1,2-dithiacyclohexane)]ClO₄, [Cu^I(**5**)]ClO₄. This compound is a bright-yellow microcrystalline solid, yield 83%. Anal. Calcd, for C₂₆H₂₆ClCuN₂O₄S₂: C 52.61, H 4.41, N 4.72%. Found: C 52.66, H 4.40, N 4.69. Mass spectra (MS-ESI, on an acetonitrile solution of a redissolved solid sample): *m/z* 493, 495 for [Cu(**5**)]⁺. ¹H NMR (CD₃CN): δ = 8.27 (d, 2H) + 8.12 (d, 2H) + 7.96 (t, 2H) + 7.62 (m, 4H) + 7.44 (d, 2H), H of the quinoline rings; 4.28 (m, 4H, S-CH₂-quinoline); 3.40 (m, 2H, (S)CHCH(S) of the cyclohexane ring); 1.9–1.3 (m, 8H, CH₂ of the cyclohexane ring).

[Cu^{II}(*cis*-*S,S'*-bis[methyl(2'-quinolyl)]-1,2-dithiacyclohexane)](CF₃SO₃)₂, [Cu^{II}(**5**)](CF₃SO₃)₂. This compound is a green microcrystalline powder, yield 60%. Anal. Calcd, for C₂₈H₂₆CuF₆N₂O₆S₄: C 39.43, H 3.31, N 3.54%. Found: C 39.44, H 3.34, N 3.49%. Mass spectra (MS-ESI, on an acetonitrile solution of a redissolved solid sample): *m/z* 642, 644 for {[Cu(**5**)](CF₃SO₃)⁺}.⁺

[Cu^I(1,6-bis(2'-quinolyl)-2,5-dithiahexane)]ClO₄, [Cu^I(**6**)]ClO₄. This compound is a deep yellow crystalline solid, yield 92%. Anal. Calcd, for C₂₂H₂₀ClCuN₂O₄S₂: C 48.93, H 3.73, N 5.19. Found: C 48.86, H 3.72, N 5.23. Mass spectra (MS-ESI, on an acetonitrile solution of a redissolved solid sample): *m/z* 439, 441 for [Cu(**6**)]⁺. ¹H NMR (CD₃CN): δ = 8.43 (d, 2H) + 8.37 (d, 2H) + 8.04 (d, 2H) + 7.74 (t, 2H) + 7.68 (t, 2H) + 7.59 (d, 2H), H of the quinoline rings; 4.38 (s, 4H, SCH₂-quinoline); 2.97 (s, 4H, SCH₂CH₂S).

[Cu^{II}(1,6-bis(2'-quinolyl)-2,5-dithiahexane)](CF₃SO₃)₂·2H₂O, [Cu^{II}(**6**)](CF₃SO₃)₂·2H₂O. This compound is a green glassy solid, yield 88%. Anal. Calcd, for C₂₄H₂₄CuF₆N₂O₈S₄: C 37.25, H 3.10, N 3.62%. Found: C 37.19, H 3.07, N 3.64%. Mass spectra (MS-ESI, on an acetonitrile solution of a redissolved solid sample): *m/z* 588, 590 for {[Cu(**6**)](CF₃SO₃)⁺}.⁺

Spectrophotometric Titrations and Determination of Complexation Constants. Titrations were performed on 30–50 mL samples (kept under a dinitrogen atmosphere) of 10⁻³ to 10⁻⁴ M solutions of ligand in CH₃CN, by microadditions of a standard CH₃-CN solution of either [Cu^I(CH₃CN)₄]ClO₄ or Cu(CF₃SO₃)₂. In a

Table 1. Crystal and Refinement Data

formula	CuN ₂ C ₂₂ S ₂ H ₂₀ ClO ₄
fw	539.5
cryst size (mm ³)	0.10 × 0.18 × 0.28
cryst syst	triclinic
space group	<i>P</i> $\bar{1}$
<i>a</i> (Å)	10.0391(13)
<i>b</i> (Å)	11.188(12)
<i>c</i> (Å)	12.0271(27)
<i>V</i> (Å ³)	1135.5(12)
<i>Z</i>	2
<i>D</i> _{calcd} (g × cm ⁻³)	1.578
<i>T</i> (K)	298(3)
<i>μ</i> (mm ⁻¹)	1.296
scan type	<i>ω</i> -2θ
θ range (deg)	2–30
abs correction method	ψ-scan
index ranges	-14 ≤ <i>h</i> ≤ 14 -15 ≤ <i>k</i> ≤ 15 0 ≤ <i>l</i> ≤ 16
reflms measured/unique	6905/6611 (<i>R</i> _{int} = 0.0241)
refinement type	<i>F</i> ²
<i>R</i> ¹ _a	0.0493
<i>R</i> _{all}	0.1313
<i>wR</i> ₂	0.0927
GOF ^b	1.019
refined params	406
weighting scheme	$w = 1/[\sigma^2(F_o^2) + (0.0356P)^2 + 0.2032P]$ where $P = (F_o^2 + 2F_c^2)/3$
(shift/esd) _{max}	0.000
max, min Δρ (e × Å ⁻³)	0.309, -0.303

^a *R*₁ = Σ||*F*_o| - |*F*_c||/Σ|*F*_o| (calculated on 721 reflections with *I* > 2σ₁).

^b GOF = $S = [\sum[w(F_o^2 - F_c^2)^2]/(n - p)]^{0.5}$.

typical experiment, 1:1 metal/ligand molar ratio was reached after addition of 20 portions of 10 μL each of the metal salt solutions. Log *K* values for complexation were obtained through nonlinear least squares refinement of titration data (absorbance vs volume of added metal cation solution) using the Hyperquad2000 package.¹¹

Electrochemistry and Spectroelectrochemistry. The apparatus for coupled controlled potential coulometry-UV-vis spectral measurements was assembled as already described.^{5b} Cyclic voltammetry studies were carried out in anhydrous CH₃CN solution, 0.1 M in (*t*-But)₄NClO₄. The working electrode was a platinum microsphere and the counter electrode a platinum wire. An SCE electrode was used as the reference, dipped in the working solution through a jacket filled with 0.1 M aqueous NaClO₄. The measured potential values were also checked by using a platinum wire as the reference electrode and by adding ferrocene to the working solution as an internal standard; the potential values referred to the Fc⁺/Fc couple can be transformed into values referred to SCE, or vice versa, considering an *E*_{1/2} value of 425 mV vs SCE, in CH₃CN, determined for the Fc⁺/Fc couple.¹²

X-ray Data Collecting and Processing. Crystal data and details on the crystallographic study are reported in Table 1.

Intensity data were obtained on an Enraf-Nonius CAD4 diffractometer, using graphite monochromated Mo Kα radiation. Unit cell parameters were obtained by least-squares fitting of 25 centered reflections monitored in the range 4.89° < θ < 10.21°. Calculations were performed with the WinGX-97 software.¹³ Corrections for

(11) Gans, P.; Sabatini, A.; Vacca, A. *Talanta* **1996**, *43*, 1739. The same kind of titrations has been carried out also in CH₂Cl₂ as solvent, finding slightly different log*K* values (Cu^I: 7.0, 6.6, 6.0; Cu^{II}: 5.8, 6.0, 5.3 for ligands **4**, **5**, and **6**, respectively). In solvents such as DMF and DMSO fast complexes decomposition is observed.

(12) Gennett, T.; Milner, D. F.; Weaver, M. J. *J. Phys. Chem.* **1985**, *89*, 2787.

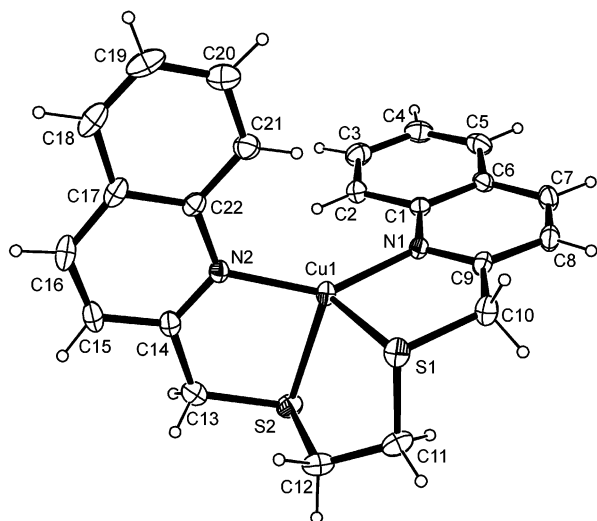


Figure 1. Molecular structure of $[\text{Cu}^{\text{I}}(\mathbf{6})](\text{ClO}_4)$. The perchlorate anion has been omitted for clarity. Selected bond distances and angles: Cu1–N1 1.986(3) Å; Cu1–N2 1.991(2) Å; Cu1–S1 2.380(2) Å; Cu1–S2 2.364(3) Å; N1–Cu1–N2 142.6(1)°; N1–Cu1–S1 87.49(9)°; N1–Cu1–S2 120.12(9)°; N2–Cu1–S1 117.08(8)°; N2–Cu1–S2 88.0(1)°; S1–Cu1–S2 93.32(7)°.

Lp and empirical absorption were applied.¹⁴ The structure was solved by direct methods (SIR92)¹⁵ and refined by full-matrix least-squares using SHELXL-97¹⁶ with anisotropic displacement parameters for all non-hydrogen atoms. Hydrogen atoms were located in the difference Fourier maps and refined with isotropic displacement parameters. Rotational disorder for one perchlorate group was detected, and two alternative positions for the oxygen atoms were refined. Atomic scattering factors were taken from *International Tables for X-ray Crystallography*.¹⁷ Diagrams of the molecular structures were produced by the ORTEP program.¹⁸

Physical Measurements. UV–vis spectra were taken on Hewlett-Packard HP8453 diode array spectrophotometer. IR spectra were carried out on a Mattson 5000-FT-IR instrument. ¹H NMR spectra were carried out on a Bruker AMX 400 spectrometer. Mass spectra (ESI) were recorded on a Finnigan MAT TSQ 700 instrument.

Results and Discussion

(1) Structure of $[\text{Cu}^{\text{I}}(\mathbf{1,6}\text{-bis}(2'\text{-quinolyl})\text{-2,5-dithiahexane})]\text{ClO}_4$. X-ray diffraction on a single crystal of the Cu^I complex of ligand **6** allowed us to determine its crystal and molecular structure, which is shown in Figure 1. It consists of monomeric $[\text{Cu}^{\text{I}}(\mathbf{6})]^+$ complexes and ClO_4^- anions which do not interact with the metal center. Copper(I) is four-coordinated, bonding to the two nitrogen atoms of the quinoline groups and to the two sulfur atoms. The overall geometry at the metal center can be described as tetrahedral, even if serious distortions are found with respect to ideal

tetrahedral geometry: in particular, the S–Cu–S angle is 93.32°, while the N–Cu–N angle is 142.6° (see Figure 1 for other significant bond angles and distances). The two quinoline rings are planar as expected; a calculation of the mean planes reveals that the mean deviations are 0.002 and 0.006 Å, respectively, for the two groups, and they form an angle of 80.9°. Rotational disorder at the perchlorate anion has been found, and two alternative positions for the oxygen atoms have been refined. The crystal packing is maintained by van der Waals forces.

(2) Cu^I Complexes in Solution. Mass spectra experiments carried out with the electron spray (ESI) technique found that Cu^I complexes of ligands **4–6** are monomeric also in solution. On redissolving solid samples of the three complexes in acetonitrile, yellow solutions are obtained, which display peaks relative to the monocharged $[\text{Cu}^{\text{I}}(\text{ligand})]^+$ molecular cations (see Experimental Section for values), while no trace of mono- or bipovalent dimeric species is evidenced. It has to be stressed that, on the contrary, the quite similar ligands **1–3** form helical dimers with Cu^I.⁵ Ligands **1–3** are too rigid to fold and coordinate a single Cu⁺ cation in a tetrahedral fashion, so that two ligands have to couple and intertwine to satisfy the requirements of Cu⁺ for tetrahedral coordination. On changing the sp²-hybridized –HC=N– moiety with the sp³-hybridized –CH₂–S–, ligands **4–6** gain flexibility with respect to **1–3**. Formation of monomeric species with Cu^I thus reflects the ability of the new ligands to fold around the Cu⁺ cation and impart to it a tetrahedral coordination, as indicated also by the molecular structure of $[\text{Cu}^{\text{I}}(\mathbf{6})]\text{ClO}_4$.¹⁹ Moreover, the similar coordination geometry at the copper center among the Cu⁺ complexes of **4–6** is supported by the similar UV–vis spectra displayed: bands are found with λ_{max} 364 nm ($\epsilon = 3050 \text{ M}^{-1} \text{ cm}^{-1}$), 350 nm ($\epsilon = 2200 \text{ M}^{-1} \text{ cm}^{-1}$), and 348 nm ($\epsilon = 2160 \text{ M}^{-1} \text{ cm}^{-1}$) in the cases of **4–6**, respectively. Also, ¹H NMR spectra determined on the Cu(I) complexes of **4–6** in CD₃CN confirm their monomeric nature. Only shifts in the position of the signals are found on passing from the free ligands to the complexes (see Experimental Section for detailed spectra description), while no change in the number or multiplicity of the signals is observed.

Spectrophotometric titration experiments were carried out by addition to a solution of the chosen ligand of substoichiometric quantities of Cu⁺ from a standard acetonitrile solution of $[\text{Cu}(\text{CH}_3\text{CN})_4]\text{ClO}_4$. Ascending linear absorbance versus equivalents of added Cu⁺ profiles were found at λ_{max} , which changed into a plateau after 1 equiv of added metal. As no changes of slope were observed in the linear ascending part, formation of species with a stoichiometry different from 1:1 can be excluded even in the presence of excess ligand with respect to Cu⁺. The formation constants for equilibria

(13) Farrugia, L. J. *WinGX-97, An integrated system of Publicly Available Windows Programs for the Solution, Refinement and Analysis of Single-Crystal X-ray Diffraction*; University of Glasgow: Glasgow, 1997.

(14) North, A. C. T.; Philips, D. C.; Mathews, F. S. *Acta Crystallogr., Sect. A* **1968**, *24*, 351.

(15) Altomare, A.; Cascarano, G.; Giacovazzo, C.; Gualardi, A. *J. Appl. Crystallogr.* **1993**, *26*, 343.

(16) Sheldrick, G. M. *SHELXL-97, Programs for Crystal Structure Analysis*; University of Göttingen: Göttingen, Germany, 1998.

(17) *International Tables for X-ray Crystallography*; Kynoch: Birmingham, England, 1974; Vol. 4, pp 99–101, 149–150.

(18) Farrugia, L. J. *J. Appl. Crystallogr.* **1997**, *30*, 565.

(19) Although we were not able to grow crystals suitable for X-ray diffraction of the Cu^I complexes of **4** and **5**, crystals of the complex of ligand **4** with the isoelectronic d¹⁰ cation Ag⁺ were obtained. The crystal and molecular structure of $[\text{Ag}(\mathbf{4})]\text{CF}_3\text{SO}_3$ were determined, and also, in this case, a monomeric $[\text{Ag}(\text{ligand})]^+$ cation was found, with Ag⁺ coordinated with a tetrahedral geometry by the N,S,S,N donor set. Amendola, V.; Fabbri, L.; Mangano, C.; Pallavicini, P.; Zema, M. Manuscript in preparation.

$\text{Cu}^+ + \text{ligand} = [\text{Cu}(\text{ligand})]^+$ are similar for **4–6**: log K values of 5.8 (± 0.1), 5.44 (± 0.03), and 4.98 (± 0.03) have been determined for **4–6**, by means of nonlinear least squares absorbance data refinement.¹¹ As the donor set is identical for the three ligands, the higher values found for the ligands containing the 1,2-cyclohexanediyil framework could indicate an higher degree of preorganization toward tetrahedral coordination in these two molecules.

A final remark has to be dedicated to the solid state and solution stability of the Cu^I complexes: in the solid, they can be stored at room temperature and in air without any apparent degradation, while acetonitrile solutions of $[\text{Cu}^I(\text{ligand})]\text{ClO}_4$ persist unchanged (as checked by UV–vis spectroscopy) for at least 24 h, even if exposed to air or moisture or even by using common, non-dry acetonitrile as solvent.

(3) Copper(II) Complexes in Solution. Formation of monomeric complexes is expected in the case of Cu^{II} , whose preference for square pyramidal or tetragonal geometries promotes the square arrangement of tetradentate ligands around the cation, with solvent molecules or anions completing the coordination sphere, as found, e.g., in the case of ligands **1–3**.^{4,5} With thio-quinoline ligands **4–6**, mass spectra ESI experiments (see Experimental Section), carried out on green acetonitrile solutions of pure, isolated $[\text{Cu}^{II}(\text{ligand})](\text{CF}_3\text{SO}_3)_2$, show the expected m/z peaks relative to $[\text{Cu}^{II}(\text{ligand})(\text{CF}_3\text{SO}_3)]^+$.²⁰ Unfortunately, we were not able to grow crystals suitable for diffraction of any of the three Cu^{II} complexes. However, in the absence of crystal and molecular structure determination, the obvious hypothesis of a square arrangement of ligands **4–6** around Cu^{2+} in solution is further corroborated by spectral data. A band in the visible zone is found for the green solutions of the $[\text{Cu}^{II}(\text{ligand})]^{2+}$ complexes, centered at 608 nm ($\epsilon = 340 \text{ M}^{-1} \text{ cm}^{-1}$), 606 nm ($\epsilon = 280 \text{ M}^{-1} \text{ cm}^{-1}$), and 628 nm ($\epsilon = 320 \text{ M}^{-1} \text{ cm}^{-1}$) for **4–6**, respectively. These values resemble closely what already found for the Cu^{II} complex of ligand **7**, which is similar to **6** but with quinoline heterocycles replaced by pyridine, and with pyridine and S groups separated by CH_2CH_2 chains instead of by CH_2 .⁶ In that case, a band centered at 605 nm ($\epsilon = 510 \text{ M}^{-1} \text{ cm}^{-1}$) was found, and in the structure, the four donors of the ligand lay in the same plane, with the copper atom somewhat displaced from it and with a further ClO_4^- anion coordinated in its apical position to give an overall square pyramidal coordination geometry. Also, the square pyramidal complex of Cu^{2+} with the macrocyclic ligand **9** displays similar spectral features, with a band centered at 646 nm and an extinction coefficient of $1154 \text{ M}^{-1} \text{ cm}^{-1}$.⁸ It is noteworthy that, in “blue copper” proteins, where the Cu^{2+} cation is coordinated with a geometry intermediate between those preferred by Cu^{II} and

(20) The presence of one triflate counteranion in the molecular cations detected by the electron spray technique is due to the formation of this ionic couple during the mass spectrum experiment and is not related to any actual coordination to Cu^{2+} of the CF_3SO_3^- anion, which is a noncoordinating one. In order to further prove this, solutions of $[\text{Cu}^{II}(\text{ligand})]^{2+}$ were electrochemically generated from $[\text{Cu}^I(\text{ligand})]\text{ClO}_4$, in 0.1 M tetrabutylammonium perchlorate, and treated with a 6-fold excess of tetrabutylammonium triflate, without observing changes in the UV–vis bands.

Table 2. E_{ox} , E_{red} , and ΔE Values ($\Delta E = E_{\text{ox}} - E_{\text{red}}$) for Both Cu^I and Cu^{II} Complexes of Ligands **4–6**^a

	E_{ox}	E_{red}	ΔE
ligand 4	975	533	442
ligand 5	1115	475	640
ligand 6	990	531	459

^a Values are reported as mV vs SCE and have been determined in CH_3CN , 0.1 M $(\text{But})_4\text{NClO}_4$, at a scan rate of $100 \text{ mV} \times \text{s}^{-1}$.

Cu^I , bands are found at similar λ values, but with distinctly different extinction coefficients (e.g., $\lambda_{\text{max}} = 595 \text{ nm}$, $\epsilon = 4500 \text{ M}^{-1} \text{ cm}^{-1}$ for plastocyanin²¹).

Also, in the case of Cu^{II} complexes the formation constants for the equilibria $\text{Cu}^{2+} + \text{ligand} = [\text{Cu}^{II}(\text{ligand})]^{2+}$ have been determined by means of spectrophotometric titrations. The obtained log K values are 6.05 (± 0.05), 6.10 (± 0.05), and 5.60 (± 0.02) for ligands **4–6**, respectively. Like in the case of Cu^I , as the ligands feature the same donor set, the similar values found for the three complexes indicate that they present a comparable preorganization degree toward a square disposition around Cu^{2+} .

As a final remark, it has to be stressed that, as in the case of Cu^I complexes, solid samples of Cu^{II} complexes with **4–6** are stable and can be stored in air at room temperature, while freshly prepared acetonitrile solutions of $[\text{Cu}^{II}(\text{ligand})](\text{CF}_3\text{SO}_3)_2$ last unchanged for at least 4–6 h, as checked by UV–vis spectroscopy, even under air and moisture exposure.²²

(4) Electrochemistry and Bistability. By the observation of the solid state and solution properties of copper complexes of ligands **4–6**, we can say that these systems are authentically bistable. For each ligand, both Cu^{II} and Cu^I complexes can be prepared and handled as solids, while their acetonitrile solutions are stable at least for hours, under the same conditions. Moreover, the log K values indicate that the ligands have such a donor set and such a flexible framework that they are capable of interacting with either Cu^{II} or Cu^I with comparable stabilities. Furthermore, the bistability of these systems is confirmed by their electrochemical behavior. Cyclic voltammetry experiments were carried out in acetonitrile solution (0.1 M TBAP as the supporting electrolyte) for both Cu^{II} and Cu^I complexes of **4–6**. Almost superimposable profiles were found for solutions of the Cu^{II} and Cu^I complexes of the same ligand. Moreover, such a large separation between the oxidation and the reduction peak was observed that the CV profiles are to be described as featuring one reduction at E_{red} potential, with no return wave, plus a separate oxidation at E_{ox} potential, again with no return wave. E_{ox} , E_{red} , and ΔE ($\Delta E = E_{\text{ox}} - E_{\text{red}}$) values are summarized in Table 2, in which they are reported as millivolts versus SCE. As an example, the CV profile of $[\text{Cu}^I(\mathbf{5})]\text{ClO}_4$ is reported in Figure 2.

These CV profiles are similar to those already found for the copper complexes of **1–3** and other related bis-imino-heterocycle ligands.^{4,5} In that case, the absence of the return

(21) Gewirth, A. A.; Solomon, E. I. *J. Am. Chem. Soc.* **1988**, *110*, 3811.

(22) After 6 h of exposition to air, not negligible spectral variations were observed. Although we did not examine the process in detail, spectral data (e.g., mass spectra) suggest the possibility that the thia-ether sulphur atoms are slowly transformed into $-\text{S}=\text{O}-$ groups.

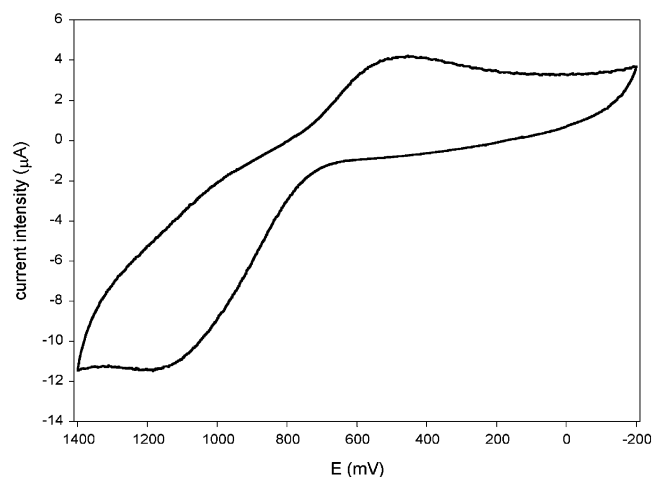


Figure 2. CV profile for $[\text{Cu}^{\text{I}}(5)]\text{ClO}_4$ obtained in acetonitrile solution, made 0.1 M in TBAP, at 200 mV/s scan rate. Potential values are referred to SCE.

wave for oxidation and reduction was due to the fast self-assembling process following the reduction of the monomeric Cu^{II} complexes and to the fast disassembling process following the oxidation of the Cu^{I} helical dimers. The copper complexes of 4–6 are instead monomeric in both oxidation states. Molecular modeling studies (MM+)²³ allow us to draw a reasonable model for the Cu^{II} complex of ligand 6: the four donors are arranged in a (distorted) square disposition around Cu^{2+} as illustrated by species II_{sq} in Scheme 1.²⁴ In the same scheme, the molecular cation $[\text{Cu}^{\text{I}}(6)]^+$, as determined by X-ray diffraction, is reproduced as species I_{tet} : it can be seen how with Cu^{I} the ligand folds to impart a tetrahedral arrangement to its four donors. On the basis of the observed CV data, the absence of the return wave for both oxidation and reduction can thus be explained by schematizing the redox behavior of the complexes with a square scheme,^{25,26} in which each electrochemical event is followed by a fast rearrangement, as in Scheme 1. The rearrangements observed after the redox events appear to be fast and complete in less than ~ 100 ms, as no return wave was observed up to a scan rate of 5 V/s.

Moreover, while each single redox event appears irreversible in the CV profile, it has to be stressed that the whole cycle is reversible, as none of the electrochemical or chemical processes bring any decomposition to the components of the system. In particular, it is possible to transform electrochemically the stable square planar Cu^{II} complexes II_{sq} into the stable tetrahedral Cu^{I} complexes I_{tet} , and then to transform

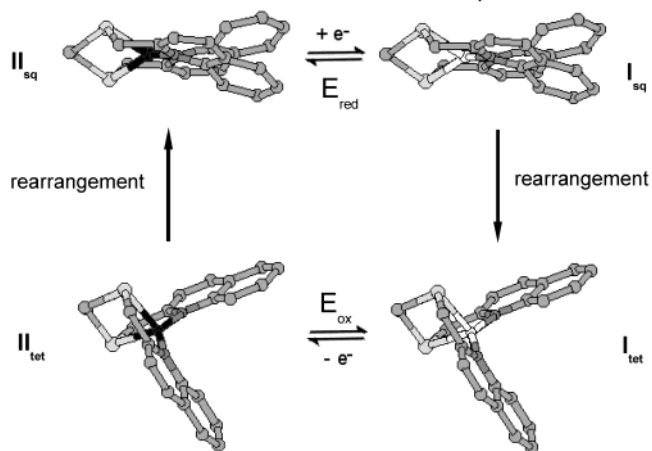
(23) Hyperchem 6.0 package.

(24) Calculations were run in acetonitrile as solvent and by considering two solvent molecules coordinated in the apical positions (omitted in the scheme). However, coordination of solvent molecules to the d^9 Cu^{2+} does not affect significantly the complex stability, as they are positioned at the apical positions of a very elongated octahedron, as an effect of the Jahn–Teller distortion. (Cotton, F. A.; Wilkinson, G. In *Advanced Inorganic Chemistry*, 5th ed.; Wiley: New York, 1988; pp 766–767.)

(25) (a) Jacq, J. *J. Electroanal. Chem.* **1971**, *29*, 149. (b) Vallat, A.; Person, L.; Roullier, L.; Laviron, E. *Inorg. Chem.* **1987**, *26*, 332.

(26) (a) Evans, D. H. *Chem. Rev.* **1990**, *90*, 739. (b) Bard, A. J.; Faulkner, L. R. *Electrochemical Methods*; Wiley: New York, 1980. (c) Villeneuve, N. M.; Schroeder, R. R.; Ochrymowycz, L. A.; Rorabacher, D. B. *Inorg. Chem.* **1997**, *36*, 4475 and references therein.

Scheme 1. Square Scheme for the Electrochemical Cycle Connecting the Stable $[\text{Cu}^{\text{I}}(6)]^+$ (I_{tet}) and $[\text{Cu}^{\text{II}}(6)]^{2+}$ Species (II_{sq})^a



^a I_{tet} is a graphically simplified version of the authentic crystal structure of $[\text{Cu}^{\text{I}}(6)]^+$, which is reported in Figure 1. The II_{sq} structure has been found for $[\text{Cu}^{\text{II}}(6)]^{2+}$ by molecular modeling calculations (MM+). Species II_{tet} and I_{sq} are drawings based on the approximation that the addition/abstraction of one electron takes place on II_{sq} and I_{tet} , respectively, with a fast process without significant structural modifications; all the molecules are displayed with aligned C11–C12 atoms

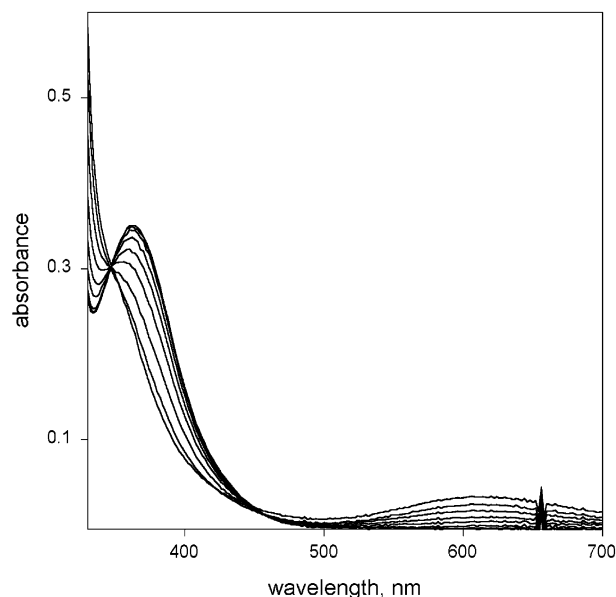


Figure 3. UV–vis spectra measured inside the working cell during the electrochemical oxidation of $[\text{Cu}^{\text{I}}(4)]\text{ClO}_4$ in acetonitrile (0.1M TBAP). The band at 364 nm (Cu^{I} , CT) decreases in intensity while the one at 608 nm (Cu^{II} , d–d) increases. The reverse series of spectra is observed when reducing the obtained $[\text{Cu}^{\text{II}}(4)]^{2+}$ solution.

it back again in the square planar Cu^{II} complex II_{sq} , without degradation, as demonstrated by controlled potential coulometry (CPC) experiments coupled with UV–vis measurements. As an example, a solution of $[\text{Cu}^{\text{I}}(4)]\text{ClO}_4$ was oxidized by setting the electrode potential at 1.0 V versus SCE (i.e., about 50 mV $> E_{\text{ox}}$), and on oxidation, the band typical of $[\text{Cu}^{\text{I}}(4)]^+$ ($\lambda_{\text{max}} = 364$ nm) decreased in intensity while the d–d band of $[\text{Cu}^{\text{II}}(4)]^{2+}$ ($\lambda_{\text{max}} = 608$ nm) increased (see Figure 3).

After the passage of ~ 1 mol of electrons per mol of Cu, no more current flow was observed, and superimposable spectra were recorded. Moreover, the final spectrum had the same features (λ_{max} and ϵ values) of that obtained from an

authentic sample of $[\text{Cu}^{\text{II}}(\mathbf{4})](\text{CF}_3\text{SO}_3)_2$. The reverse process was observed by setting the potential at 450 mV versus SCE (about $100 \text{ mV} < E_{\text{red}}$): the bands of the Cu^{II} complex decreased in intensity, those of Cu^{I} increased, and after the passage of 1 mol of electrons per mol of Cu, the original $[\text{Cu}^{\text{I}}(\mathbf{4})]^+$ spectrum was restored. The whole cycle has been repeated for all the complexes up to four times, without observing significant variations in the final spectra. As in the case of the copper complexes of ligands **1–3** and related systems, the system can thus exist in two forms in the same potential interval (e.g., $950 \text{ mV vs SCE} < E < 550 \text{ mV vs SCE}$ in the case of ligand **4**), and it can be switched from one form to the other by reaching the potential values at the edges of the bistability interval. According to this, also the systems made of ligands **4–6** and $\text{Cu}^{\text{II}}/\text{Cu}^{\text{I}}$ present electrochemical hysteresis.

A final comment is worthwhile on the values of the oxidation and reduction potentials reported in Table 1. Comparison has to be done with what is found in the literature for similar systems. For the already mentioned bis-thia-bis-pyridine ligand **7**, a reversible signal with $E_{1/2} = 555 \text{ mV}$ versus SCE was found for the reduction of the square pyramidal Cu^{II} complex, in 0.1 M aqueous KNO_3 ²⁷ (peak separation = 117 mV). In the quite rigid, dinucleating thia-imino macrocycle **8**, for the oxidation of both Cu^+ cations a value of 1096 mV versus SCE has been found, in CH_3CN 0.1 M in TBAP. Significantly, in this case the Cu^+ cations are tetrahedrally coordinated, and peak separation is that typical of a completely reversible process. Finally, in the case of the bis-imino-bis-thia macrocycle **9**, an $E_{1/2}$ value of 775 mV versus SCE is reported, in CH_3CN (NaBF_4 as supporting electrolyte) for the Cu^{I} complex.²⁸ Interestingly, the Cu^{I} complex is tetrahedral, and oxidation and reduction

peaks appear separated as in our systems, with a peak separation of 360 mV, which is explained by the authors with the serious rearrangements taking place after the redox events (according to this, the CV profile can be described as featuring an oxidation peak at 955 mV and a reduction peak at 595 mV vs SCE). With our systems, E_{red} is similar to what was found for the reduction of the square pyramidal Cu^{II} complex of ligand **7**, while E_{ox} is close to what was found for the oxidation of the tetrahedral complexes of ligands **8** and **9**.

Conclusions

The complexes of ligands **4–6** are monomeric both with Cu^{I} and Cu^{II} , so that no electrochemical self-assembling or disassembling processes are observed. However, the significant and fast rearrangements following oxidation and reduction allow also in our systems the separation of the reduction and oxidation processes, even on the faster CV time scale. According to this, these new systems are bistable and present electrochemical hysteresis.

Acknowledgment. This work was supported by the European Union (RT Network Molecular Level Devices and Machines—Contract HPRN-CT-2000-00029), and by the Italian Ministry of University and Research (PRIN—Progetto ‘Dispositivi Supramolecolari’).

Supporting Information Available: Listings of final atomic coordinates, anisotropic thermal parameters, all bond lengths and angles, intermolecular contacts, and unit cell and packing diagrams for the crystal and molecular structure of $[\text{Cu}^{\text{I}}(\mathbf{6})](\text{ClO}_4)$ in CIF format. This material is available free of charge via the Internet at <http://pubs.acs.org>.

IC025690H

(27) Authors report a value of 0.577 V vs Ag/AgCl electrode; conversion of the value referred to SCE was done by considering the Ag/AgCl couple at 0.222 mV vs NHE.

(28) Authors report a value of 0.69 V for $E_{1/2}$, and, for comparison, an $E_{1/2}$ value of 0.34 V for ferrocene, under the same conditions. The potential value has been referred by us to SCE, by considering the usual 0.425 V vs SCE value for the Fc^+/Fc couple, in acetonitrile.